

Chapter 2

Flight Path Optimization at Constant Altitude

Mark D. Ardema and Bryan C. Asuncion

Abstract In this chapter we consider flight optimization at constant altitude for a variety of missions and propulsion systems and then focus on maximizing the range of a turbofan-powered aircraft. Most analyses of optimal transport aircraft flight begin with the assumption that the flight profile consists of three segments – climb, cruise, and descent. Indeed, this is the flight profile of all long-haul commercial flights today. The dominant stage of such flights, in terms of flight time, is the cruise segment. The air transportation industry is extremely competitive and even small changes in aircraft performance have significant impacts on the operation costs of airlines. Thus, there has been, and continues to be, great interest in optimizing the cruising flight of transport aircraft.

2.1 Introduction

In this chapter we consider flight optimization at constant altitude for a variety of missions and propulsion systems and then focus on maximizing the range of a turbofan-powered aircraft. Most analyses of optimal transport aircraft flight begin with the assumption that the flight profile consists of three segments – climb, cruise, and descent. Indeed, this is the flight profile of all long-haul commercial flights today. The dominant stage of such flights, in terms of flight time, is the cruise segment. The air transportation industry is extremely competitive and even small changes in aircraft performance have significant impacts on the operation costs of

Mark D. Ardema
Santa Clara University, 500 El Camino Real Santa Clara, CA 95053, USA,
e-mail: mardema@scu.edu

Bryan C. Asuncion
Santa Clara University, 500 El Camino Real Santa Clara, CA 95053, USA,
e-mail: basuncion@scu.edu

airlines. Thus, there has been, and continues to be, great interest in optimizing the cruising flight of transport aircraft.

The classical performance relation for cruising flight is the “Brequet range equation.” This is based on steady flight (constant speed and altitude), leaving only the range and mass as dynamic variables. Integrating the state equations associated with these two variables, assuming a constant lift-to-drag ratio, gives the Brequet equation:

$$R = B \ln \frac{m_0}{m_f} \quad (2.1)$$

where R is the range, m_0 is the initial mass, m_f is the final mass, and B is the Brequet factor, given by

$$B = \frac{\lambda V}{gC} \quad (2.2)$$

where λ is the lift-to-drag ratio, V the cruise speed, g the gravitational acceleration, and C the thrust-specific fuel consumption.

Thus, to optimize the flight path (in the sense of either maximizing range for a given mass ratio or maximizing the mass ratio for a given range), a search is conducted to find the point in the flight envelope (the portion of the (h, V) plane that does not violate any constraints) that maximizes B . Because the Brequet factor changes as fuel is burned off during the flight, the optimal (h, V) values change as well. Typically the optimum altitude increases during the flight, resulting in a steady “cruise climb.” Air traffic control requires that aircrafts hold specific altitudes; thus, the operational flight paths of long-haul transport aircraft are “step climbs” during which the altitude is increased at discrete times. Note that a cruise or step climb violates the assumption of flight at constant h but the rate of change of altitude is quite small.

Several authors have used more detailed math models to study aircraft cruise, models in which V and h are allowed to vary [1, 2]. These authors have investigated whether or not cyclic cruise is better than steady cruise. It was found that flight paths with large periodic changes in h , V , and throttle could be more fuel efficient for fixed-range missions. However, the improvement (reduction) in fuel consumption was very small, 1% at best. Furthermore, such flight paths would not be compatible with air traffic procedures as the altitude oscillations sometimes exceed 10,000 ft.

On the other hand, for endurance missions (maximum time) the non-steady flight paths gave great improvement relative to steady ones.

The work just discussed focuses on the interplay between h , V , and throttle setting. Because of the operational restrictions on cruise altitude, in the present chapter we look at aircraft cruise from a different point of view; in particular, we study the interplay between aircraft mass and speed at constant altitude. This problem was first considered by Miele [3] for rocket-powered aircraft. In [4] we extended these results to jet aircraft and made some preliminary calculations. This chapter extends these results further to other types of missions and propulsion systems. Because this is a singular optimal control problem, we begin with a review of that subject.

2.2 Singular Optimal Control

Consider a system whose math model is a set of state equations:

$$\dot{x} = f(x) + g(x)u \quad (2.3)$$

where $x \in \mathfrak{R}^n$ is the state vector and $u \in \mathfrak{R}$ is the scalar control variable bounded by $u_m \leq u \leq u_M$. The state may be free or fixed at $t = 0$ and $t = t_f$. It is desired to minimize

$$J = \int_0^{t_f} [f_0(x) + g_0(x)u] dt \quad (2.4)$$

This is a problem of singular optimal control [5, 6].

In [4] we found the singular arc in two different ways – by applying the maximum principle and using Green's theorem – and found that the Green's theorem approach was much easier and hence we use this method here. Application of Green's theorem to this type of problem was introduced independently by Miele [7] and Mancill [8]. These two works are quite different; Mancill approaches the problem as an identically non-regular problem of the calculus of variations, whereas Miele approaches it as a problem of optimal control. The method was developed into a powerful analytic tool by Miele [9]. The Green's theorem method only applies to the case of two state variables, say x and y , the case considered later in the chapter.

Now consider the optimization problem with x and y fixed at $t = 0$ and $t = t_f$:

$$\begin{aligned} \dot{x} &= f_x(x, y) + g_y(x, y)u \\ \dot{y} &= f_y(x, y) + g_x(x, y)u \\ J &= \int_0^{t_f} f_0(x, y) dt \end{aligned} \quad (2.5)$$

Eliminating the control between the state equations and substituting into the cost functional results in

$$J = \int_{(x_0, y_0)}^{(x_f, y_f)} (A dx + B dy) \quad (2.6)$$

where

$$A = \frac{f_0 g_y}{f_x g_y - f_y g_x}, \quad B = \frac{f_0 g_x}{f_y g_x - f_x g_y} \quad (2.7)$$

Equation (2.6) is a line integral in the plane. Green's theorem relates line integrals around closed curves to area integrals. To use the theorem, consider the closed curve consisting of the curve to be optimized, C_1 , plus a fixed, but arbitrary, curve, C_2 , returning to the starting point; then Green's theorem is

$$\int_{C_1} (A dx + B dy) + \int_{C_2} (A dx + B dy) = \iint_A \left(\frac{\partial A}{\partial y} - \frac{\partial B}{\partial x} \right) dA \quad (2.8)$$

Since integral C_2 is fixed, minimizing integral C_1 is the same as minimizing the integral A . The critical curve associated with the latter integral is

$$\frac{\partial A}{\partial y} - \frac{\partial B}{\partial x} = 0 \quad (2.9)$$

and is optimizing. This equation is the singular arc.

2.3 The Cruise Problem

Consider an aircraft flying at constant altitude at a constant heading. The equations of motion are

$$\begin{cases} \dot{V} = \frac{T-D}{m} \dot{m} = -\beta \\ L = mg \end{cases} \quad (2.10)$$

where V is the speed; m is the mass; T , D , and L are the thrust, drag, and lift forces, respectively, and β is the fuel flow rate. It is assumed that

$$\begin{aligned} T(V) &= \Pi T_M(V) \\ \beta(V) &= C(V) T(V) \\ D &= AV^2 + \frac{BL^2}{V^2} \end{aligned} \quad (2.11)$$

where D represents a parabolic drag polar [13], $A = C_{D0} \frac{\rho s}{2}$, and $B = \frac{2K}{\rho s}$. The zero-lift drag coefficient, C_{D0} , the induced drag coefficient, K , the air density, ρ , and the reference area, s , are all taken as positive constants, a good assumption for flight at constant altitude of a subsonic aircraft. Π is the throttle setting where $\Pi_m \leq \Pi \leq 1$. In this chapter we consider three types of propulsion systems: rockets, jets, and internal combustion with propeller. Rockets are modeled by taking $C = \text{constant}$. Props are modeled by $C = (C_p/k)V$ where C_p and k are engine and propeller efficiencies, respectively. For low-speed flight ($M < 0.5$) C_p and k are nearly constant. For jet engines, C depends on various temperatures and pressures within the engine. In this chapter, we use EngineSim 19.11 to model the relationship between C and h , V , and Π .

It is desired to minimize

$$J = \int_0^{t_f} (E - V) dt \quad (2.12)$$

with t_f free. This is a problem with two states, V and m , and one control, Π . This cost functional is a weighted sum of minimum time and maximum range, with E being the weighting function. It has been found that this cost functional is closely related to direct operating cost. Special cases are maximum range ($E = 0$) and maximum endurance ($E = -8$). This is very similar to the problem first considered by Miele [3] and later appearing in Leitmann [5]. The differences are that instead of a rocket engine with constant exhaust exit velocity, we include air breathing engines with speed-dependent maximum thrust, T_M , and specific fuel consumption, C , and consider a more general cost functional.

To use Green's theorem, we begin by eliminating the control from Eq. (2.10) and substituting the result into Eq. (2.12); the result is

$$J = \int_0^{t_f} \left[(V-E) \frac{m}{D} DV + (V-E) \frac{1}{CD} dm \right] \quad (2.13)$$

Applying Green's theorem, this is equivalent to

$$J = \iint_A \left[\frac{\partial}{\partial m} \left((V-E) \frac{m}{D} \right) - \frac{\partial}{\partial V} \left((V-E) \frac{1}{CD} \right) \right] dV dm \quad (2.14)$$

Thus the singular arc is

$$\frac{\partial}{\partial m} \left[\left((V-E) \frac{m}{D} \right) \right] - \frac{\partial}{\partial V} \left[\left((V-E) \frac{1}{CD} \right) \right] = 0 \quad (2.15)$$

There are three special cases depending on propulsion system and mission:

Jet (Range):

$$m = \frac{V^2}{g} \sqrt{\frac{A(1+CV + \frac{V}{C}C_v)}{B(3+CV - \frac{V}{C}C_v)}}$$

Jet (Endurance):

$$m = \frac{V^2}{g} \sqrt{\frac{A(2+CV + \frac{V}{C}C_v)}{B(2+CV - \frac{V}{C}C_v)}}$$

Rocket (Range):

$$m = \frac{V^2}{g} \sqrt{\frac{A(1+CV)}{B(3+CV)}} \quad (2.16)$$

Rocket (Endurance):

$$m = \frac{V^2}{g} \sqrt{\frac{A}{B}}$$

Prop (Range):

$$m = \frac{V^2}{g} \sqrt{\frac{A(1+CV + \frac{C_p V}{kC})}{B(3+CV - \frac{C_p V}{kC})}}$$

Prop (Endurance):

$$m = \frac{V^2}{g} \sqrt{\frac{A(2+CV + \frac{C_p V}{kC})}{B(2+CV - \frac{C_p V}{kC})}}$$

There is a second-order necessary condition which optimal singular control must satisfy. The traditional approach uses the maximum principle to identify the switching function and then the switching function is differentiated until the control appears. This was done in [4] and great algebraic complexity was encountered.

However, [11] gives a Green's theorem approach to this condition and we use this here. The condition for the endurance mission is

$$\frac{\partial^2}{\partial V^2} \left(\frac{1}{CD} \right) \geq \frac{\partial^2}{\partial m \partial V} \left(\frac{m}{D} \right) \quad (2.17)$$

Carrying out the differentiation for a rocket engine gives

$$\begin{aligned} &6A^2C^2V^2 - 18AC^2Em^2V^{-2} + 2C^2E^2m^4V^{-6} - 6Em^2V^{-2}C^2A \\ &+ 4C_vCA^2V^3 - 4C_vCA^2V^3 - 4C_vCE^2m^4V^{-5} - C_{vv}CA^2V^4 \\ &- C_{vv}C2AE m^2 - C_{vv}CE^2m^4V^{-4} + 2C_v^2A^2V^4 + 4C_v^2AE m^2 \\ &+ 2C_v^2E^2m^4V^{-4} \geq 12Em^2V^{-1}AC^3 - 4E^2m^4V^{-5}C^3 \\ &+ 2E^2m^4V^{-5}C^3 \end{aligned} \quad (2.18)$$

where subscripts denote partial derivatives.

2.4 Fanjet Specific Fuel Consumption

Aircraft data show that specific fuel consumption is far from constant and can vary significantly over an aircraft's flight envelope. The equations for C are very complicated and highly specific to the engine. C is mainly a function of speed and air temperature. Altitude is a factor in C calculation, because air temperature varies with altitude.

For turbojets and turbofans, C depends on several temperatures in the engine, pressure ratios, bypass ratios, and the fuel to air mass ratio in the combustor. There are computer simulation capabilities that can provide the information we want, and here we use the NASA Glenn EngineSim [11].

The NASA Glenn EngineSim, setup for a CF6 turbofan sized for use on a 747-400, was sampled at various velocities to generate a C vs. V relationship for full throttle of the engine. Another condition was generated, where the engine thrust matches the drag of the aircraft with respect to speed, which is more accurate to what an engine mounted on an aircraft would provide. This was done by developing a table of speed and parabolic drag values, entering the speed into EngineSim, and then adjusting the throttle to match the drag.

Figure 2.1 shows these results for the general relation of C as a function of speed at constant altitude. The dashed line represents the full throttle condition, and as expected, the slower the aircraft is flying, the more efficient the turbofan becomes. The solid line represents the change to specific fuel consumption if in addition to the reduced speed, the throttle is reduced to match the drag. Notice that minimum throttle occurs at about 250 m/s.

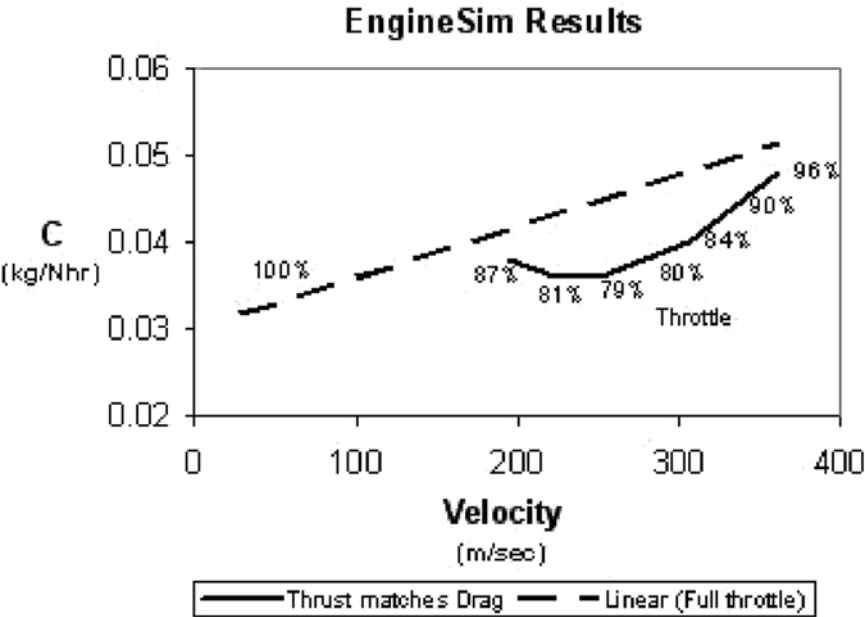


Fig. 2.1 C variation with respect to speed for a high-bypass turbofan

It is possible to simplify Eq. (2.16), max range with the jet, by considering values of the VC term. Subsonic aircraft speed does not get much above 300 m/s; however, C can vary significantly depending on the type of engine and application. As will be discussed later in this chapter, the CF6-80C2 engine example would have a C around 0.04 kg/N hr, which would be around 10^{-5} s/m. Therefore, its VC , a dimensionless number, would be on the order of 3×10^{-3} , which is small compared to 1 and 3. To give an order of scale to the VC value, the Concorde flying at Mach 2 only has a VC value of 0.018. The VC for an F-16 at full afterburner is around 0.03. For the VC term to be really large, the aircraft would need to have high speed and be using rocket engines. The Space Shuttle main engines have a VC of 1.67.¹ These numbers are summarized in Table 2.1. Thus the VC term may be neglected for our application.

Table 2.1 Magnitude of VC term with various aircrafts

Subsonic Jet	0.003
Concorde	0.02
F-16	0.03
Space Shuttle	1.7

¹ The Space Shuttle VC value is approximated by orbital speed divided by specific impulse and gravity. Specific impulse for the Space Shuttle Main Engines (SSME) is 428 s.

2.5 An Example

For example calculations, we choose a maximum range mission with a fanjet-powered aircraft for which the first of Eq. (2.16) applies. The aircraft selected is a Boeing 747-400 with General Electric CF6-80C2 high bypass, multistage, turbofan engines. Depending on the options installed on the engine, the CF6-80C2 is rated to produce max thrust of 282,500 N per engine (63,500 lbf) [12] at sea level.

The design range of a 747-400 is listed as 13,444 km (8,354 mi.), with a maximum takeoff mass of 362,875 kg (800,000 lb) [13, 14]. At takeoff, a full fuel load would be 120,205 kg (265,000 lb). This leaves 61,415 kg (135,400 lb) for passengers, crew, and cargo. It is easy to see that even small percentage changes to the amount of fuel required for each flight can provide significant potential for increased payload and thus for cost savings and increased revenue.

For the 747-400 aircraft and CF6-80C2 engine model, we input speed and throttle values to get C , thereby getting an order of magnitude of C_V to determine if it is significant or not. By using two mass–speed points, entering them into EngineSim, adjusting throttle, and looking at the change of C , we find C_V is on the order of 10^{-8} . With V/C being on the order of 10^8 , the term $(V/C)C_V$ is significant. Therefore, after eliminating VC , but leaving $(V/C)C_V$, the first of Eq. (2.16) becomes

$$m = \frac{V^2}{g} \sqrt{\frac{A \left(1 + \frac{V}{C} C_V\right)}{B \left(3 - \frac{V}{C} C_V\right)}} \quad (2.19)$$

Using EngineSim $(V/C)C_V$ is found to vary from 1.21 to 0.93 for the aircraft/engine combination considered here.

Equation (2.19) is plotted in Fig. 2.2 for various altitudes. The main feature is that the speed decreases as fuel is burned off.

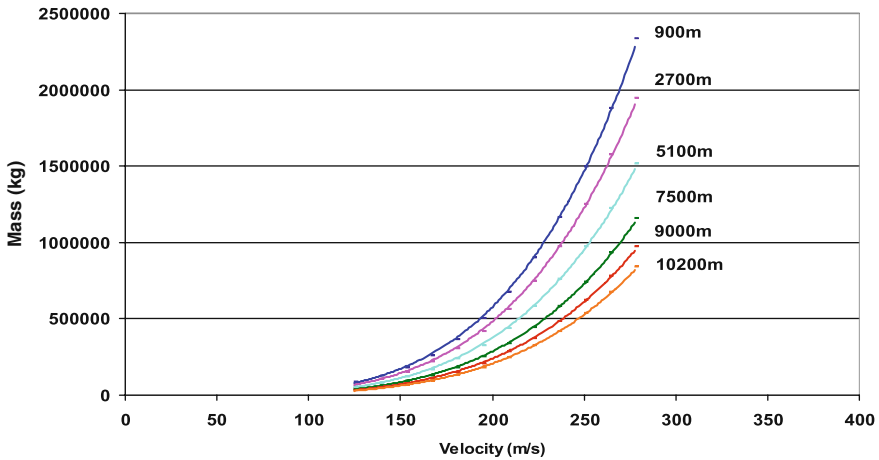


Fig. 2.2 Singular arcs and optimal path for 747-400 at different altitudes

Table 2.2 Comparative results for optimal path and standard cruise

Flight profile	Cruise speed (m/s)	Altitude (m)	Range (km)	Flight time (hrs)
Standard steady cruise	250	10,000	13,570	15.1
Optimal steady cruise	210	9,000	14,889	19.7
Optimal singular arc	219–206	9,800	14,904	19.5

We now conjecture how optimal paths look in the (m,V) plane. The aircraft climbs to the start of the cruise on the singular arc, follows the arc until cruise fuel is expended, and then descends. For our example, the entire cruise portion of the flight may follow the singular arc. A 747-400 with maximum fuel load flying the singular arc path for the entire cruise portion of the flight starts out burning about 10.0 kg/km and finishes burning 6.60 kg/km. In contrast, the standard steady speed path at the cruise speed of 250 m/s would start out burning 10.4 kg/km and finish burning 7.62 kg/km.

A computer simulation of the flight’s cruise portion shows that following the singular arc would result in an additional range. The steady cruise is performed at 250 m/s at 10,000 m altitude. The optimal singular arc is performed at 219–206 m/s at 9800 m altitude. With the results from Table 2.2, it can be observed that the optimal singular arc could have a maximum range of 14,904 km and a travel time of 19.50 hr.

Because many airlines’ costs are directly related to flight time, transport aircraft actually fly faster than the speed for maximum range with a given fuel load (equivalently minimum fuel for a given range). Thus, to make the comparison with singular flight fair, we maximized range in steady cruise. The results are included in Table 2.2. Optimal steady cruise is at 210 m/s speed and 9,000 m altitude. Optimal singular arc flight covers 115 more miles than optimal cruising flight, probably within the noise band of the numerical calculations.

Time history plots (Figs. 2.3, 2.4, 2.5 and 2.6) compare the optimal singular arc path with that for standard cruise in terms of speed, range, mass, and thrust,

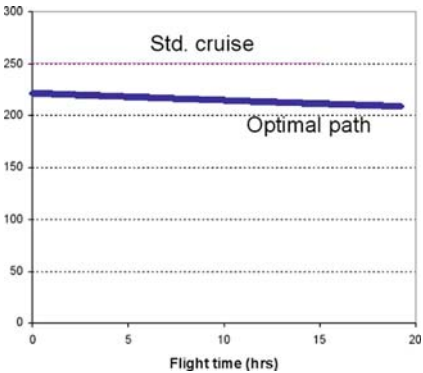


Fig. 2.3 Comparative time history plots of optimal path and standard cruise in terms of speed

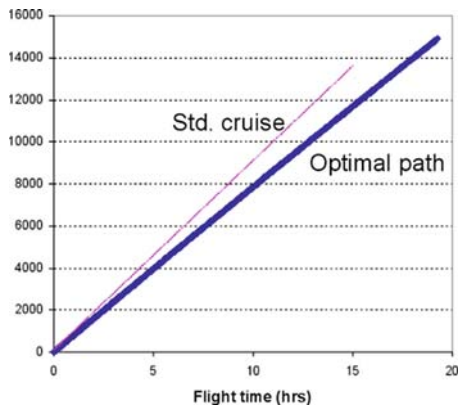


Fig. 2.4 Comparative time history plots of optimal path and standard cruise in terms of range

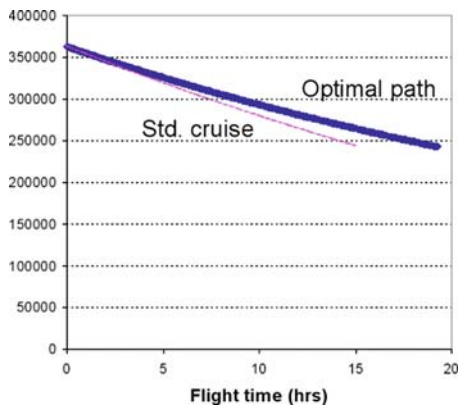


Fig. 2.5 Comparative time history plots of optimal path and standard cruise in terms of mass

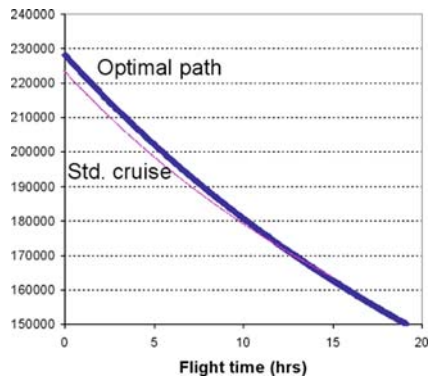


Fig. 2.6 Comparative time history plots of optimal path and standard cruise in terms of thrust

respectively. One interesting finding is that the optimal path results in higher thrust during the entire flight time. This would tend to disagree with the fuel savings finding, except that the aircraft is flying at a more efficient speed for the large turbofan engines. Because of this, the engines require less fuel to produce each unit of thrust and can therefore consume less fuel per unit distance flown even though the thrust is greater than for the standard cruise.

2.6 Conclusions and Discussion

We have analyzed aircraft cruise at constant altitude with a model with mass and speed as state variables. This is a singular optimal control problem and we have identified the singular arc for a weighted sum of time and range for a variety of propulsion systems. The singular arcs have been specified for six special cases; the combinations of endurance (maximum time) and maximum range for three propulsion systems: rockets, turbo and fanjets, and internal combustion/propeller. Example calculations using the Boeing 747-400 with General Electric CF6-80C2 engines for the maximum range mission show potential large savings in fuel. However, if steady cruise is optimized to maximize range, the difference in range between steady and singular arc flight is very small. In spite of this discouraging result, there are interesting avenues for future research.

First, the singular arcs of other propulsion systems need to be determined and evaluated numerically. Second, the endurance mission needs to be investigated. In view of the fact that non-steady flight paths have shown significant improvements relative to steady ones, there could be big improvements in flying singular arc paths. Third, the second-order necessary condition needs to be derived and numerically evaluated for all missions and propulsion systems.

Further study is required to determine the fuel consumption, range, and time over an entire flight. The boundary conditions on the cruise portion of the flight are different from the steady cruise case. For example, for the range mission, the singular arc cruise ends at a lower speed than it begins and thus the range gained in descent will be shorter. Thus the fuel consumption in climb and descent must be added to give a fair comparison.

There are obvious air traffic control issues with flying singular arc flight paths in controlled airspace. Mixing singular arc paths with steady cruise paths is clearly not acceptable. Even with all aircraft flying singular arc paths there is the issue of separating aircraft that is decelerating. In many parts of the world, however, airspace is not controlled and flight time is not critical. In such situations, singular arc flight may be employed immediately.

Perhaps the most important application of our results is to aircraft design. Key aircraft parameters (such as wing loading, aspect ratio, and wing sweep) could be chosen to move the singular arc to its optimum location in the mass-speed plane. The performance criteria should be a suitably weighted combination of fuel consumption and flight time so as to minimize direct operating cost.

Acknowledgments The authors thank Doug Pargett for the use of his computer program and for valuable discussions. We also thank P.K. Menon for suggesting the endurance mission and for pointing out the paper by Mancill.

References

1. Menon, P.K., Study of Aircraft Cruise, *Journal of Guidance, Control and Dynamics*, Vol. 12, No. 5, Sept–Oct 1989, pp. 631–639.
2. Sachs, G. and Christodoulou, T., Reducing Fuel Consumption of Subsonic Aircraft by Optimal Cyclic Cruise, *Journal of Aircraft*, Vol.24, No.9, 1987, pp. 616–622.
3. Miele, A., *The Calculus of Variations in Applied Aerodynamics and Flight Mechanics*, Optimization Techniques, edited by G. Leitmann, Academic Press, New York, 1962, pp. 100–171.
4. Pargett, Douglas and Ardema, Mark, *Flight Path Optimization at Constant Altitude*, Santa Clara University.
5. Leitmann, G., *The Calculus of Variations and Optimal Control*, Plenum Press, New York, 1981, pp. 225–237.
6. Bryson, A. and Ho, Y., *Applied Optimal Control*, Taylor and Francis, New York, 1975, pp. 246–270.
7. Miele, A., Problems of Minimum Time in Nonsteady Flight of Aircraft, *Atti della Accademia delle Scienze di Torino, Classe di Scienze Fisiche, Matematiche e Naturali*, Vol. 85, 1951, pp. 41–52.
8. Mancill, J. D., Identically Non-Regular Problems in the Calculus of Variations, *Mathematica Y Fisca Teorica*, Universidad Nacional del Tucuman, Republica Argentina, Vol.7, No.2, June 1950, pp. 131–139.
9. Miele, A., Extremization of Linear Integrals by Green's Theorem, *Optimization Techniques*, edited by G. Leitmann, Academic Press, New York, 1962, pp. 69–99.
10. Holt, Ashley, *Engineering Analysis of Flight Vehicles*, Addison-Wesley, New York, 1974, pp. 113–114.
11. NASA Glenn EngineSim, Ver. 1.6e [online application] <http://www.grc.nasa.gov/WWW/K-12/airplane/ngnsim.html> [cited 2 December 2004].
12. General Electric Aircraft Engines website: GE Transportation Aircraft Engines: CF6.: <http://www.geae.com/engines/commercial/cf6/cf6-80c2.html> [cited 2 December 2004].
13. Boeing Aircraft Company website: Boeing 747 Family <http://www.boeing.com/commercial/747family/technology.html> [cited 2 December 2004].
14. Jane's All the World's Aircraft 1997-98, 1988-89, Jane's Information Group Limited, Sentinel House, 1998.

Variational Analysis and Aerospace Engineering

Buttazzo, G.; Frediani, A.

2009, XXVI, 518 p. 300 illus. in color., Hardcover

ISBN: 978-0-387-95856-9